

Ultrafast dynamics in Fe₆₅Co₃₅ alloys: Effect of Re doping

R. S. Malik and R. Knut

*Department of Physics and Astronomy,
Uppsala University, Box 516, SE-751 20, Uppsala, Sweden*

R. Gupta, A. Kumar, and P. Svedlindh

*Department of Materials Science and Engineering,
Uppsala University, Box 534, SE-75121, Uppsala, Sweden*

R. Stefanuik, Y. O. Kvashnin, J. Söderström, and O. Karis

*Department of Physics and Astronomy,
Uppsala University, Box 516, SE-75120, Uppsala, Sweden*

O. Eriksson

*Department of Physics and Astronomy, Uppsala University,
Box 516, SE-75120, Uppsala, Sweden and*

School of Science and Technology, Örebro University, SE-70182 Örebro, Sweden

Abstract

The soft magnetic FeCo alloys are of interest due to their potential applications in magnetic recording heads, spin valves and, magnetic tunneling junctions. The magnetic damping parameter plays a vital role in the performance of these spintronics devices. The α parameter increase in these alloys with doping of $5d$ elements. Here, we have investigated the effect of Re doping on the element-specific magnetization dynamics of Ru/Fe₆₅Co₃₅/Ru thin films using time-resolved magneto-optical Kerr effect. By varying the concentration of Re from 0% to 12.6 %, no change of demagnetization time constant is observed. However, a gradual change of the remagnetization time constant is observed with the increase of Re concentration. This remagnetization dynamics can be related to the Gilbert damping parameter (α) of these films. An interesting time-resolved dynamics at the Ru-edge is observed. A significant increase of asymmetry (% 40) signal is observed for a undoped sample and drops down with the Re doping. This effect is possibly due to a combine interface effect of capped Ru layer and FeCo film.

I. INTRODUCTION

Since the discovery of ultrafast demagnetization by Beaurepaire *et al.* in 1996 that ferromagnetic Ni film can be demagnetized on a subpicosecond time scale by fs laser pulse excitation¹, laser induced magnetization dynamics received a growing attention. After more than two decades, complete understanding of the microscopic processes governing magnetization dynamics is still elusive. The possibility of optically manipulating the magnetization on such a fast time scale offered many potential applications from technology prospective. Beside technological relevance, research in this area led to discover new interesting phenomena like all-optical magnetization switching, transfer of angular terahertz spin currents and optical inter-site spin transfer (OISTR) effect²⁻⁶. Experimentally it has been observed that the 3d (Fe,Co, Ni) ferromagnets as well as their alloys and several half-metallic systems show the characteristic demagnetization times within the 100 fs time scale⁷⁻¹³. However, 4f (Tb and Gd) ferromagnets show much more complex two-step demagnetization¹⁴.

Koopmans *et al.* have proposed a demagnetization model inspired by the Elliot-Yafet (EY) spin-flip scattering mediated by impurities¹⁵. Employing theoretical calculation, an analytical expression that connects the demagnetization time constant τ_M with the Gilbert damping parameter α via the Curie temperature T_C . In the EY theory, the spin-flip probability is given by the amount of spin mixing of the electronic wave function which is determined by the spin-orbit coupling strength. The studies have demonstrated that the damping parameter of transition metals and their alloys can be modified by introducing 3d and 5d transition metals or rare earth elements¹⁶⁻¹⁸. The doping of 5d in transition metal alloys can increase α parameter due to a large spin-orbit coupling, which in turn influences the demagnetization time τ_M of these alloys. Walowski *et al.* measured the demagnetization dynamics of Permalloy doped with a transition and rare earth elements. While α increases with doping, a constant τ_M is observed¹⁹. Radu *et al.* showed in a similar study that the dynamics of Permalloy doped with rare earth elements (Ho, Dy, Tb and Gd) shows both an increase of demagnetization and remagnetization time constant²⁰.

The soft magnetic FeCo alloys are promising materials for high frequency spintronic application due to their high magnetization saturation (M_s), high permeability and thermal stability²¹⁻²³. A high damping parameter can be required in order to increase the fast switching time in magnetic memory devices. The magnetic damping parameter plays a vital role for the performance of these spintronic devices. One drawback of FeCo alloys can be their high coercivity (H_c) which can be solved by growing the film on suitable buffer layers^{24,25}.

In this letter, the ultrafast magnetization dynamics of Fe₆₅Co₃₅ films with Re doped are studied. The table-top HHG setup provides extreme ultraviolet (XUV) photons in 40-72 eV energy range. The advantage of using HHG is that it can provide element-specific information in magnetic alloys. The polycrystalline Fe₆₅Co₃₅ films doped with Re are deposited at room temperature by using magnetron sputtering. First a 3 nm seed layer of Ru is deposited on Si (100)/SiO₂ substrate. Ru seed layer is used to decrease the coercivity and effective damping of the film. After seed layer, a 20 nm thick Re-doped Fe₆₅Co₃₅ film is deposited. The Re concentration (0 - 12.6 at. %) are varied by changing the deposition rate of Re. Finally, a 3 nm capping layer Ru layer is deposited. These films have body-centered-cubic (bcc) structure. The distribution of the doping within the films was characterized by Rutherford backscattering (RBS). The lattice constant increases with increasing of Re doping and follows the trend from theoretical calculation shown previously in Ref.²⁶. The

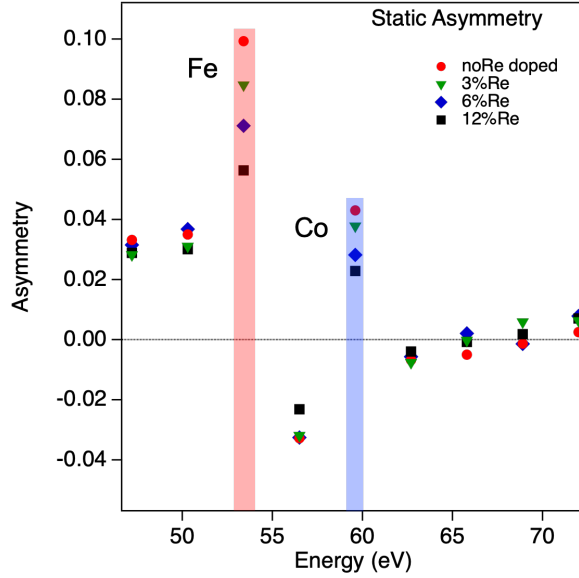


FIG. 1. Measured static asymmetries $A(E)$ in Ru/FeCo/Ru samples with different concentration of Re doping in a T-MOKE spectrometer. The red shaded region represent the asymmetry of Fe at 54 eV and blue region for Co asymmetry at 60 eV.

detailed description of the deposition process and structural characterization of these films are describe in earlier studies^{26,27}.

The ultrafast magnetization dynamics measurements of Ru/Fe₆₅Co₃₅/Ru thin films are carried out by using a transverse magneto-optical Kerr (T-MOKE) pump-probe setup²⁸. The laser system is a chirped pulse amplification (CPA)²⁹, system running at a central wavelength of 800 nm with a maximum energy of 2 mJ per pulse and a length of 35 fs. The laser beam is split into two parts; 80% of the laser beam is used for generating the extreme-ultraviolet (XUV) probe beam and 20% is used as a pump beam. The XUV probe beam is generated by focusing laser light into a gas cell filled with helium through a process called high harmonics generation (HHG)^{30,31}. This HHG process provide photons in 40 – 72 eV energies range. The incident angle between the sample and the probe beam is fixed at 45° in order to get maximum magnetic signal in the T-MOKE geometry^{32,33}. The delay between pump and probe beam is controlled by a delay stage. An electromagnet with a magnetic field strength of ± 80 mT is used to saturate the sample. The pump and probe are generated from the same laser pulse and the temporal jitter between them is effectively eliminated. The details description of the experimental setup has been reported in^{28,34}.

In the T-MOKE spectrometer, the sample is magnetized perpendicularly to the plane of incidence of the incoming p-polarized light. The reflected light from the sample is recorded with a charged-coupled device (CCD) camera. In order to detect the T-MOKE signal, the change in reflective intensities at the absorption edges of Fe and Co were recorded for two opposite orientations of magnetic field. This asymmetry $A(E)$ is the ratio of difference of reflected intensities for two magnetization directions according to Eq.1:

$$A = \frac{I_p^{(+)} - I_p^{(-)}}{I_p^{(+)} + I_p^{(-)}}, \quad (1)$$

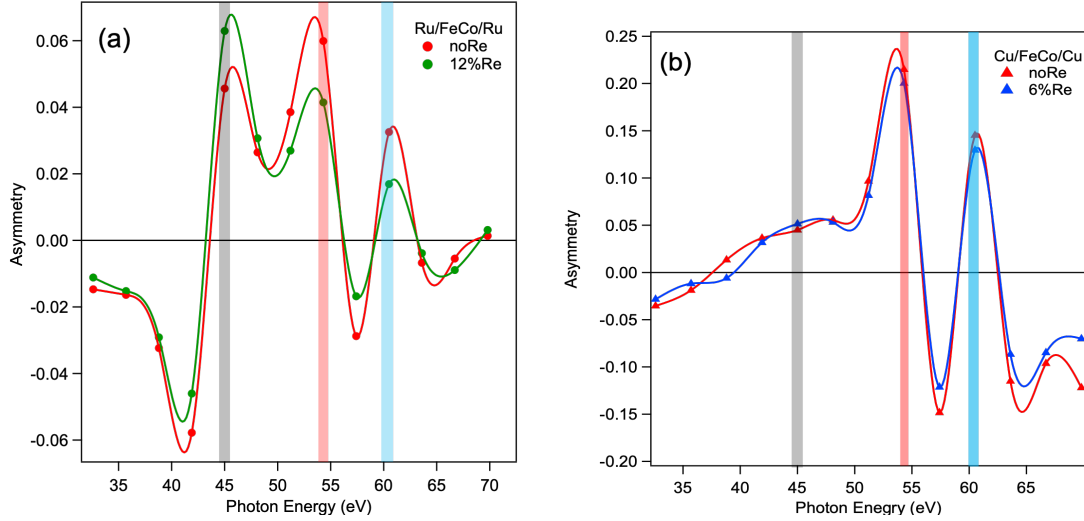


FIG. 2. (a) Static asymmetries of Ru/FeCo/Ru samples in a broad energy range of 32 - 72 eV. The different shaded regions represent the absorption edges of Ru (grey), Fe (red) and, for Co (blue) respectively. The red curve represent the asymmetry of no Re doped and green curve is for 12% Re doped sample (b) The measured asymmetry in Cu/FeCo/Cu samples with capping layer of Cu is shown.

where $I_p^{(+)}$ and $I_p^{(-)}$ are the reflected intensities measured for two different magnetization direction. The Fig.1 shows the measured static asymmetries in Ru/FeCo/Ru thin films with different concentration of Re. In a undoped sample, a strong asymmetry signal is observed (red circle) at the M-absorption edge of Fe (~ 54 eV) and for Co (~ 60 eV) respectively. This asymmetry which is assumed to be proportional to the magnetization and already discussed in previous studies^{12,32,35}. The asymmetry $A(E)$ is measured in reflection geometry with a Transverse magneto-optical Kerr effect (T-MOKE) spectrometer^{28,34}. As the Re concentration increases, this asymmetry (A) decreases monotonously for both Fe and Co. The saturation magnetization of these films decrease about 35% with increasing Re doping upto 12.6 at.% reported in Ref.²⁷.

II. RESULTS AND DISCUSSION

The Fig. 2(a) shows the measured static asymmetry of two Ru/FeCo/Ru samples with a seed and capping layer of Ru. The red curve is the measured asymmetry of sample with no doping and green curve is for 12% Re doping. The red shaded region is asymmetry of Fe at the absorption edge and blue region for Co asymmetry. Interestingly, We also observed a asymmetry signal at the 44 eV energy (grey region). This signal is coming from the Ru layer, since Ru has a N-absorption edge in this energy range. To verify this asymmetry, we have measured the static asymmetry of similar Cu/FeCo/Cu samples with a seed and capping layer of Cu. There is a weak asymmetry signal at 44 eV, which is possibly coming from Fe. Since Fe has a broad asymmetry energy range. Another interesting observation is that there is no significant effect of doping in the $A(E)$. In both samples, no doped (blue curve) and 6% Re doped (black curve), the asymmetries of Fe and Co are almost similar.

We have studied the ultrafast magnetization dynamics of FeCo films as a function of Re

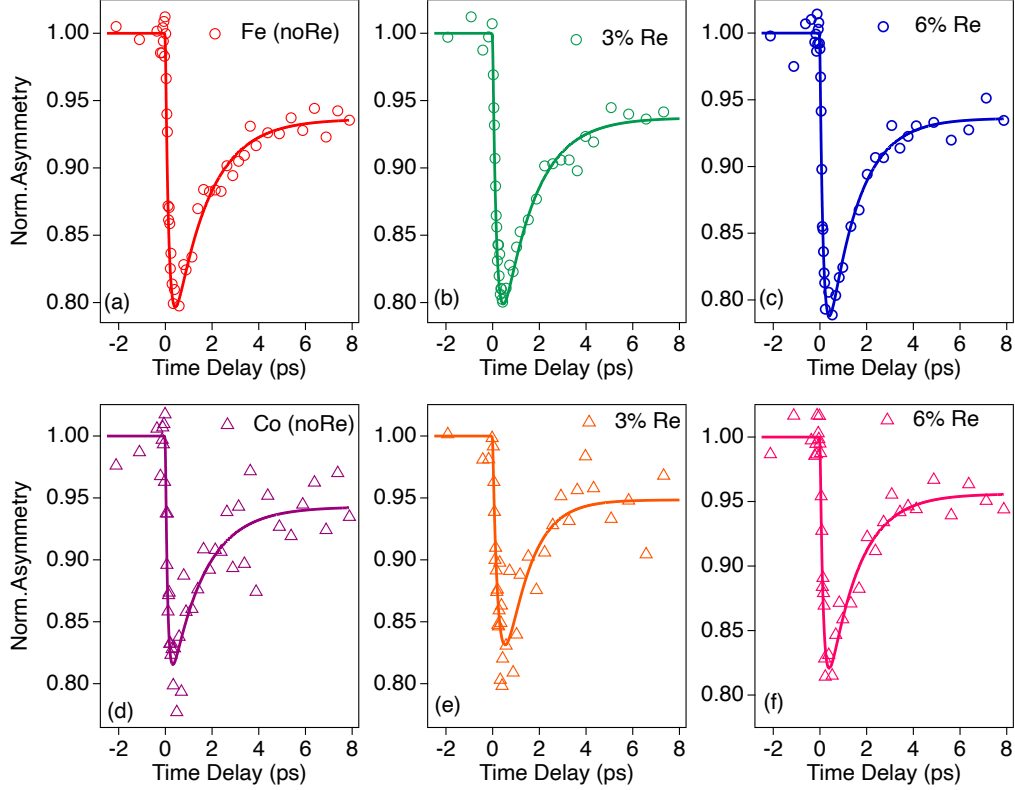


FIG. 3. Ultra fast magnetization dynamics of Ru/FeCo/Ru films with different concentration of Re doping. (a-c) are the time resolved the dynamics of Fe shown with empty circle. (d-f) are the dynamics of Co shown with empty triangle respectively. The empty circles (Fe) and triangles (Co) are the experimental measured data points and solid lines are the fitting curve

doping. Fig. 3 (a-f) shows the element-specific magnetization dynamics of Fe and Co for different concentration of Re doping. The empty circle (Fe) and triangles (Co) represent the experimental data measured in a time-resolved magneto-optical Kerr effect (TR-MOKE) spectrometer respectively. The x-axis is the time delay between pump (IR) and probe (XUV) pulses and the y-axis is the normalized asymmetry. The negative time delay is the time when the probe pulse is arrive before the pump. Time zero is when both pump and probe pulses are spatially and temporally overlap on the sample. The positive time delay is the time when the pump pulse come before the probe pulse. In all samples, the pump fluence is maintained, so that all samples shows about similar amount of demagnetization (% 20). The experimental data is fitted using the analytical solution of the three temperature model described in Ref.³⁶. The important fitting parameters are extracted, such as demagnetization τ_M and remagnetization τ_R times.

In Fig. 3 (a) shows the dynamics of Fe in a undoped sample, (b) in 3% Re doped and (c) in a 6% Re doped sample respectively. In all three samples, Fe shows a rapid demagnetization within few hundreds femtoseconds (fs). After that, it start to recover the initial magnetization on a longer time scale. Note that in all samples, the magnetaton is not fully recovered up to 8 ps. Similarly, In Fig. 3,(d) shows the ultrafast dynamics of Co in sample with no Re, (e) dynamics in a 3% Re doped and (f) dynamics in a 6% Re

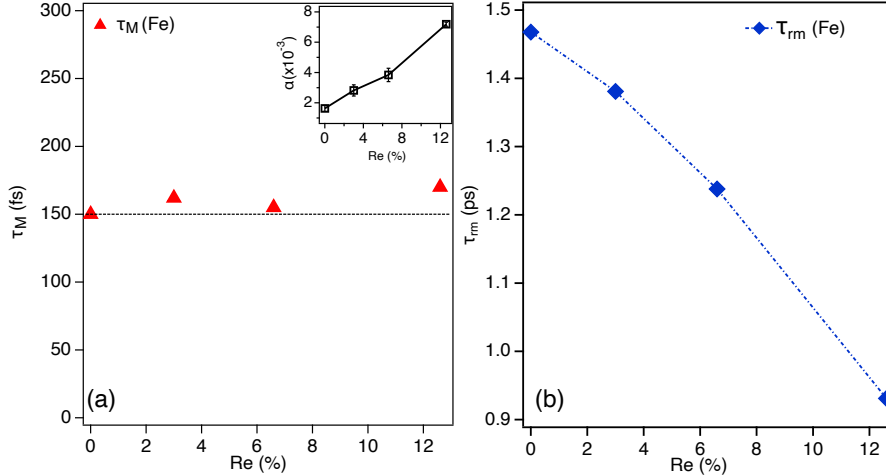


FIG. 4. (a) Demagnetization τ_M time of Fe with different Re content is shown. The inset shows the variation of Gilbert damping parameter (α) with different concentration of Re as measured by FMR. The black line is guides to the eye (b) Measured remagnetization τ_R time of Fe is shown. The dotte blue line is guided to the eye.

doped sample respectively. The amount of Co demagnetization is slightly smaller in 3% Re doped and 6% Re as compared to Fe dynamics. Note that the experimental data of Co is quite scatter with comparison to Fe. One of the possible reason for noisy data is the less composition of Co in the film. To have a good comparison of Co dynamics with Fe, more experiment statistics are needed.

Its has been shown previously that the Gilbert damping (α) enhanced significantly with Re doping in $\text{Fe}_{65}\text{Co}_{35}$ films^{26?}. This α increases with the increase of Re doping concentration. Koopman *et.al* described a theoretically model that qualitatively relate the demagnetization dynamics τ_M to the Gilbert damping via Curie temperature¹⁵. The model predicted that the demagnetization mechanism can enhance due to the impurity-assisted spin-flip scattering processes. However, Radu. *et.al* showed that the magnetization dynamics of Permalloy (Py) doped with rare earth (4f) does not show any agreement with the model. In another study of Py doped with transition metal and rare earth doping showed that a significant change in damping is observed with doping but the demagnetization times remains the same¹⁹.

In Fig. 4 (a) the measured demagnetization dynamics of Fe for different concentration of Re are shown. The inset show the increase of Gilbert damping parameter for different Re concentration. Interestingly, the demagnetization time τ_{dm} for Fe is similar for in all Re-doped FeCo films and does not affected by the α parameter. However, on a longer time scale, a different remagnetization dynamics of Fe are observed in all four samples and shows in Fig. 4 (b). For a sample with out Re doping, a longer remagnetization time τ_{rm} is observed which indicate that the recovery of the magnetization takes place slowly. This slowly relaxation dynamics are possibly due to the low damping of the system. As the Re doping increases in the film, faster relaxation dynamics of Fe are observed. Note that the difference in τ_{rm} time with change of α is not so big in first three samples. However, in sample with 12.6 Re doping, the value of α increase by a factor two and corresponding abrupt change in τ_{rm} time is observed. There is one to one correspondence of damping

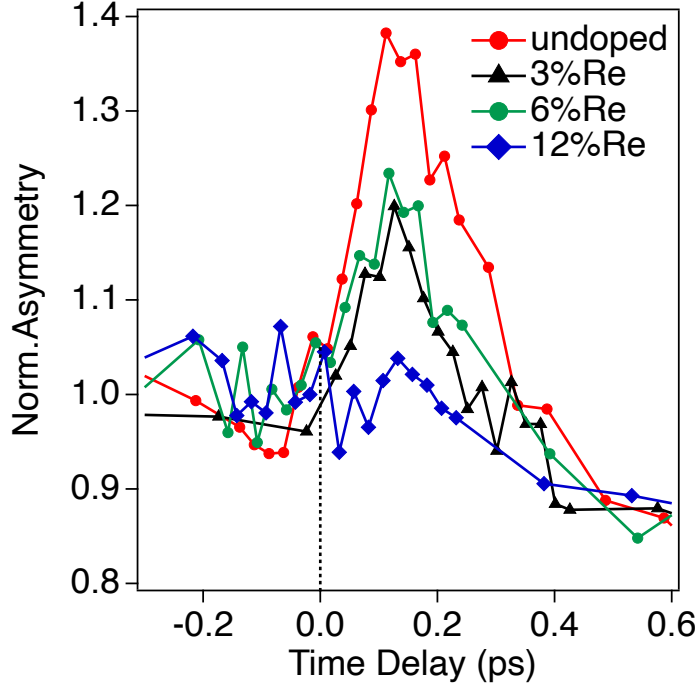


FIG. 5. Ultrafast magnetization dynamics of Ru in FeCo films are shown. A increase in the asymmetry signal is observed around time zero (dotted line). This asymmetry is strongest for undoped sample (red curve) and decreases with the increase of Re doping.

with the remagnetization dynamics of Fe in Re-doped FeCo films. In case of Co, a similar dynamics during demagnetization and remagnetization are also expected. Due to the poor statistics of Co as shown in Fig. 3 (d-f), we can not compare dynamics of Co with Fe dynamics.

In all four FeCo thin films, 3 nm Ru is used as a seed and capping layer. Ru has a absorption $N_{2,3}$ edge around this energy range and at this energy, a unique ultrafast dynamics of Ru is observed and shown in in Fig.5. Around time zero, there is a about 40 % enhancement of asymmetry signal with opposite sign is observed. This asymmetry signal is very strong in a undoped sample (red curve). For samples with 3 % and 6 % Re doping, this enhance asymmetry signal is same but less stronger as compare to the undoped sampled. However in 12 % doped sample, there is no enhancement of asymmetry signal is observed (blue curve). To quantify this effect, either it is a Ru effect or combine interface effect between Ru and FeCo layer. We have measured the time resolved dynamics of FeCo film capped with a 5 nm Cu layer. In the static asymmetries of Cu/FeCo/Cu samples in Fig.2 (b), there is very weak asymmetry observed around 44 eV which is possibly a effect of Fe. Interesting, in the time resolved dynamics of FeCo with no Re doped sample, no enhancement of the asymmetry signal is observed at this energy.

A similar effect is also investigated in Ref.³⁷, where the ultrafast dynamics at the Co/Cu interface are probed for different thicknesses of Co. (0.4-10nm). The films up to 3 nm show the strong demagnetization. For larger thick film, the magnetization reverses its sign. The possible explanation for this inhomogeneous magnetization dynamics is due to competing

laser induced spin transport and spin-flip scattering mechanism.

- ¹ E. Beaurepaire, J.-C. Merle, A. Daunois, and J.-Y. Bigot, Phys. Rev. Lett. **76**, 4250 (1996).
- ² C. Stanciu, F. Hansteen, A. Kimel, A. Kirilyuk, A. Tsukamoto, A. Itoh, and T. Rasing, Physical review letters **99**, 047601 (2007).
- ³ A. Schellekens, K. Kuiper, R. De Wit, and B. Koopmans, Nature communications **5**, 1 (2014).
- ⁴ D. Rudolf, C. La-O-Vorakiat, M. Battiato, R. Adam, J. M. Shaw, E. Turgut, P. Maldonado, S. Mathias, P. Grychtol, H. T. Nembach, T. J. Silva, M. Aeschlimann, H. C. Kapteyn, M. M. Murnane, C. M. Schneider, and P. M. Oppeneer, Nat. Commun. **3**, 1037 (2012).
- ⁵ T. Seifert, U. Martens, S. Günther, M. Schoen, F. Radu, X. Chen, I. Lucas, R. Ramos, M. H. Aguirre, P. A. Algarabel, *et al.*, in *Spin*, Vol. 7 (World Scientific, 2017) p. 1740010.
- ⁶ P. Tengdin, C. Gentry, A. Blonsky, D. Zusin, M. Gerrity, L. Hellbrück, M. Hofherr, J. Shaw, Y. Kvashnin, E. K. Delczeg-Czirjak, M. Arora, H. Nembach, T. J. Silva, S. Mathias, M. Aeschlimann, H. C. Kapteyn, D. Thonig, K. Koumpouras, O. Eriksson, and M. M. Murnane, Sci. Adv. **6** (2020).
- ⁷ E. Carpene, E. Mancini, C. Dallera, M. Brenna, E. Puppini, and S. De Silvestri, Phys. Rev. B **78**, 174422 (2008).
- ⁸ M. Cinchetti, M. Sánchez Albaneda, D. Hoffmann, T. Roth, J.-P. Wüstenberg, M. Krauß, O. Andreyev, H. C. Schneider, M. Bauer, and M. Aeschlimann, Phys. Rev. Lett. **97**, 177201 (2006).
- ⁹ C. Stamm, T. Kachel, N. Pontius, R. Mitzner, T. Quast, K. Holldack, S. Khan, C. Lupulescu, E. Aziz, M. Wietstruk, *et al.*, Nat. Mater. **6**, 740 (2007).
- ¹⁰ M. Wietstruk, A. Melnikov, C. Stamm, T. Kachel, N. Pontius, M. Sultan, C. Gahl, M. Weinelt, H. A. Dürr, and U. Bovensiepen, Phys. Rev. Lett. **106**, 127401 (2011).
- ¹¹ G. M. Müller, J. Walowski, M. Djordjevic, G.-X. Miao, A. Gupta, A. V. Ramos, K. Gehrke, V. Moshnyaga, K. Samwer, J. Schmalhorst, *et al.*, Nature Materials **8**, 56 (2009).
- ¹² C. La-O-Vorakiat, E. Turgut, C. A. Teale, H. C. Kapteyn, M. M. Murnane, S. Mathias, M. Aeschlimann, C. M. Schneider, J. M. Shaw, H. T. Nembach, and T. J. Silva, Phys. Rev. X **2**, 011005 (2012).
- ¹³ .
- ¹⁴ B. Koopmans, G. Malinowski, F. Dalla Longa, D. Steiauf, M. Fähnle, T. Roth, M. Cinchetti, and M. Aeschlimann, Nat. Mater. **9**, 259 (2010).
- ¹⁵ B. Koopmans, J. J. M. Ruigrok, F. D. DallaLonga, and W. J. M. de Jonge, Phys. Rev. Lett. **95**, 267207 (2005).
- ¹⁶ A. Rebei and J. Hohlfeld, Physical review letters **97**, 117601 (2006).
- ¹⁷ J. Rantschler, R. McMichael, A. Castillo, A. Shapiro, W. Egelhoff Jr, B. Maranville, D. Pugalurtha, A. Chen, and L. Connors, Journal of applied physics **101**, 033911 (2007).
- ¹⁸ G. Woltersdorf, M. Kiessling, G. Meyer, J.-U. Thiele, and C. Back, Physical review letters **102**, 257602 (2009).
- ¹⁹ J. Walowski, G. Müller, M. Djordjevic, M. Münzenberg, M. Kläui, C. A. F. Vaz, and J. A. C. Bland, Phys. Rev. Lett. **101**, 237401 (2008).
- ²⁰ I. Radu, G. Woltersdorf, M. Kiessling, A. Melnikov, U. Bovensiepen, J.-U. Thiele, and C. H. Back, Physical review letters **102**, 117201 (2009).
- ²¹ H. Fukuzawa, K. Koi, H. Tomita, H. N. Fuke, H. Iwasaki, and M. Sashiki, Journal of applied

- physics **91**, 6684 (2002).
- ²² N. Sun and S. Wang, IEEE transactions on magnetics **36**, 2506 (2000).
- ²³ M. Takagishi, H. Fuke, S. Hashimoto, H. Iwasaki, S. Kawasaki, R. Shiozaki, and M. Sahashi, Journal of Applied Physics **105**, 07B725 (2009).
- ²⁴ A. Hashimoto, K. Hirata, T. Matsuu, S. Saito, and S. Nakagawa, IEEE Transactions on Magnetism **44**, 3899 (2008).
- ²⁵ M. C. Hickey and J. S. Moodera, Physical review letters **102**, 137601 (2009).
- ²⁶ S. Akansel, A. Kumar, V. A. Venugopal, R. Esteban-Puyuelo, R. Banerjee, C. Autieri, R. Brucas, N. Behera, M. A. Sortica, D. Primetzhofer, *et al.*, Physical Review B **99**, 174408 (2019).
- ²⁷ R. Gupta, N. Behera, V. A. Venugopal, S. Basu, A. K. Puri, P. Ström, M. A. Gubbins, L. Bergqvist, R. Brucas, P. Svedlindh, and A. Kumar, Phys. Rev. B **101**, 024401 (2020).
- ²⁸ S. Jana, J. A. Terschlüsen, R. Stefanuik, S. Plogmaker, S. Troisi, R. S. Malik, M. Svanqvist, R. Knut, J. Söderström, and O. Karis, Rev. Sci. Instrum. **88**, 033113 (2017).
- ²⁹ D. Strickland and G. Mourou, Opt. Commun. **55**, 447 (1985).
- ³⁰ M. Lewenstein, P. Balcou, M. Y. Ivanov, A. L’huillier, and P. B. Corkum, Phys. Rev. A. **49**, 2117 (1994).
- ³¹ P. B. Corkum, Phys. Rev. Lett. **71**, 1994 (1993).
- ³² S. Mathias, C. La-O-Vorakiat, P. Grychtol, P. Granitzka, E. Turgut, J. M. Shaw, R. Adam, H. T. Nembach, M. E. Siemens, S. Eich, C. M. Schneider, T. J. Silva, M. Aeschlimann, M. M. Murnane, and H. C. Kapteyn, Proc. Natl. Acad. Sci. USA. **109**, 4792 (2012).
- ³³ M. Hecker, P. M. Oppeneer, S. Valencia, H.-C. Mertins, and C. M. Schneider, J. Electron Spectrosc. Relat. Phenom. **144**, 881 (2005).
- ³⁴ S. Plogmaker, J. A. Terschlüsen, N. Krebs, M. Svanqvist, J. Forsberg, U. B. Cappel, J.-E. Rubensson, H. Siegbahn, and J. Söderström, Rev. Sci. Instrum. **86**, 123107 (2015).
- ³⁵ S. Mathias, C. La-O-Vorakiat, J. M. Shaw, E. Turgut, P. Grychtol, R. Adam, D. Rudolf, H. T. Nembach, T. J. Silva, M. Aeschlimann, C. M. Schneider, H. C. Kapteyn, and M. M. Murnane, Journal of Electron Spectroscopy and Related Phenomena **189**, 164 (2013).
- ³⁶ U. Atxitia, O. Chubykalo-Fesenko, J. Walowski, A. Mann, and M. Münzenberg, Phys. Rev. B **81**, 174401 (2010).
- ³⁷ J. Chen, J. Wiczorek, A. Eschenlohr, S. Xiao, A. Tarasevitch, and U. Bovensiepen, Applied Physics Letters **110**, 092407 (2017).